Journal of Sound and Vibration (2002) **251**(3), 395–408
doi:10.1006/jsvi.2001.4001, available online at http://www.idealibrary.com on IDEAL®

OPTIMAL GAIN DISTRIBUTION FOR TWO-DIMENSIONAL MODAL TRANSDUCER AND ITS IMPLEMENTATION USING MULTI-LAYERED PVDF FILMS

J. KIM AND J.-K. RYOU

Agency for Defense Development, Taejon, Korea

AND

S. J. KIM

Department of Aerospace Engineering, Seoul National University, Seoul, 151-742, *Korea.*
E-mail: *seungjok@snu.ac.kr*

(*Received* 17 *October* 2000, *and in final form* 31 *July* 2001)

Using finite element techniques to optimize the spatial gain distribution of PVDF film, we developed a modal transducer for specific modes to perform real-time vibration control of integrated smart structures. This method makes it possible to design the modal transducer for two-dimensional structure with arbitrary geometry and boundary conditions. As a practical means for implementation, the gain distribution was approximated by optimizing electrode patterns, lamination angles, and relative poling directions of the multi-layered PVDF transducer. This corresponds to the approximation of a continuous function using discrete values. A genetic algorithm was used in the optimization of the electrode pattern and lamination angle of each PVDF layer. For this purpose, the continuous value of the lamination angle was encoded into discrete values using binary 5-bit strings. Validity of the proposed concept was demonstrated experimentally. A modal sensor for the first and second modes of cantilevered composite plate was designed using two layers of PVDF films. The experimental results show that spillover signals by residual modes were successfully reduced using the optimized multi-layered PVDF sensor. The actuator was designed also using two layers of PVDF films to minimize the system energy in the control modes. Real-time vibration control system was successfully realized using the optimized sensor, actuator, and a discrete LQG controller. Closed-loop test showed that modal peaks of the first and second modes were reduced by amounts of 13 and 4 dB respectively.

1. INTRODUCTION

In the active vibration control of structures, limitations of the on-board computer and modelling errors of the system practically restricted control to a few critical modes. This introduces control and observation spillover [1] due to the residual (uncontrolled) modes, which can lead to instability in the closed-loop system. The adverse effects of the spillover can be prevented by using special control schemes [2] or by introducing modal transducers [3]. Modal transducers will sense or actuate the modes that were taken into consideration in the design, thus eliminating any instability from the residual modes. To create modal transducers using discrete point transducers, signals obtained from different locations must be processed simultaneously. The considerable amount of signal processing required

0022-460X/02/130395 + 14 $35.00/0

reduces the robustness of the control loop. In contrast to the discrete point transducers, the distributed piezoelectric transducers perform signal processing by using the charge collecting phenomenon of piezoelectric materials to implement modal transducer in spatial domain. Thus, the distributed piezoelectric transducers have a relative advantage over the discrete point transducers. Due to the easiness of electrode pattern shaping and the flexibility and lightness of the polyvinylidene fluoride (PVDF), it has been widely used as distributed transducers. Most research related to PVDF has been focused on the design of the electrode patterns of PVDF transducers.

Lee [4] established the concept of using PVDF film for the distributed modal transducer. He implemented it on a one-dimensional beam structure by making the width of the effective electrode proportional to the second derivative of a particular mode shape. Burke and Hubbard [5] studied the effects of spatial gain distribution of the distributed transducer for control of vibration in two-dimensional structures. Miller *et al.* [6] developed an algorithm to determine the specific piezoelectric field distributions required to implement modal transducers in the anisotropic rectangular plates. Sullivan *et al.* [7] designed the "all-mode" transducers for simply supported rectangular plates using gain-weighted, shaped distributed piezoelectric transducers. In the case of one-dimensional structures, the continuous gain distribution can be obtained by inspecting the mode shape of the structure. The gain distribution can be easily implemented by varying the width of the PVDF film along the primary axis of the structure [3, 8]. However, in the case of the two-dimensional structures, there is no general method for obtaining the continuous gain distribution required for implementation of modal transducers, excluding a few structures with simple geometric shapes and boundary conditions. Even if the required gain distribution is obtained, there is no practical method for implementing the gain distribution. In our previous work [9], modal transducer for the two-dimensional structure was obtained by optimizing electrode pattern of the PVDF film. However, the final shape of the optimized electrode pattern could not be explained because there were no data about the required continuous gain distribution.

We developed a method based on finite elements, which enabled us to determine the optimal spatial gain distribution required to create modal transducers for the specific modes of two-dimensional structures. There were no limitations of the geometric shapes and boundary conditions of the structure because this method was based on FEM. If this optimal gain distribution could be implemented on a real structure, its performance as a modal transducer would be optimal. Still, it is not easy to spatially vary the gain of PVDF film. So, as a practical means for implementing the optimal gain distribution, the gain distribution was approximated by optimizing electrode patterns, lamination angles, and poling directions of the multi-layered PVDF transducers. Simply put, this procedure can be viewed as the approximation of a continuous function using discrete values.

2. OPTIMAL GAIN DISTRIBUTION

2.1. MODAL TRANSDUCER IN TWO-DIMENTIONAL STRUCTURE

Using the sensor equation [4], the amount of induced charge q in a piezoelectric sensor was

$$q(t) = -z\int_S G(x, y)\left[\bar{e}_{31}\frac{\partial^2 w}{\partial x^2} + \bar{e}_{32}\frac{\partial^2 w}{\partial y^2} + 2\bar{e}_{36}\frac{\partial^2 w}{\partial x \partial y}\right] \mathrm{d}S, \tag{1}$$

where z is the distance from neutral plane to mid-plane of the sensor, $\bar{e}_{ij}$'s are the piezoelectric constants in the laminate axes, S is the effective area of sensor covered with the electrode, w is the lateral displacement, and $G(x, y)$ is the spatial gain distribution of the piezoelectric sensor. The lateral displacement, w, can be decomposed into the modal summation

$$w(x, y, t) = \sum_{k=1}^{\infty} \phi_k(x, y)\eta_k(t), \tag{2}$$

where $\phi_k(x, y)$ is the kth mode shape of the structure and $\eta_k(t)$ is the kth modal co-ordinate. Substituting equation (2) into equation (1), q_k, the charge induced by the kth mode shape can be defined as

$$q_k(t) = -z\int_S G(x, y)\left[\bar{e}_{31}\frac{\partial^2\phi_k}{\partial x^2} + \bar{e}_{32}\frac{\partial^2\phi_k}{\partial y^2} + 2\bar{e}_{36}\frac{\partial^2\phi_k}{\partial x\partial y}\right]\mathrm{d}S$$

$$= -z\int_S G(x, y)f_k(x, y)\,\mathrm{d}S. \tag{3}$$

In equation (3), if the spatial gain distribution $G(x, y)$ is designed to be orthogonal to all $f_k(x, y)$'s except $f_j(x, y)$, one can obtain the modal transducer for the jth mode. In one- and two-dimensional structures with simple geometry and boundary conditions, $G(x, y)$ for the specific modal transducer can be obtained using the analytic method. However, designing the modal transducer based on the analytical method has limitations when the geometric shapes and boundary conditions of the structure are complicated. In the following sections, the general method of obtaining the optimal gain distribution will be introduced.

2.2. FINITE ELEMENT MODEL

The finite element method was used to model the composite plate integrated with the piezoelectric sensor and actuator. Four-node Kirchhoff plate elements were used [10]. There are three degrees of freedom (d.o.f.) at each node, namely, the component of displacement normal to the plane of the plate, w, and two rotations $\theta_x = \partial w/\partial y$ and $\theta_y = -\partial w/\partial x$. The spatial gain distribution is modelled to have a constant value $G^{(e)}$ within each element. The transverse displacement, w, was interpolated in the form of

$$w = \sum_{j=1}^{12} \Delta_j\psi_j(x, y), \tag{4}$$

where Δ_j denotes the nodal values of w and its derivatives, and $\psi_j(x, y)$ are the Hermite interpolation functions. Using equation (4), equation (1) can be discretized as follows:

$$q(t) = \sum_e z\int_{S^{(e)}}\left[-\sum_{j=1}^{12}\left(e_{31}\frac{\partial^2\psi_j}{\partial x^2} + e_{32}\frac{\partial^2\psi_j}{\partial y^2} + 2e_{36}\frac{\partial^2\psi_j}{\partial x\partial y}\right)\Delta_j\right]\mathrm{d}S\; G^{(e)}$$

$$= \sum_e \mathbf{U}^{(e)\mathrm{T}}\left(\int_{S^{(e)}}\mathbf{B}^{(e)\mathrm{T}}\mathbf{e}\;\mathrm{d}S\right)G^{(e)}, \tag{5}$$

where the superscript e denotes the element, $\mathbf{U}$ is the nodal d.o.f. vector, $\mathbf{B}^{(e)}$ is the interpolation matrix of the in-plane strain, and $\mathbf{e}$ is the piezoelectric constants vector.

Equation (5) can also be expressed in the simple matrix form by defining

$$\mathbf{Q}^{(e)} = \int_{S^{(e)}} \mathbf{B}^{(e)\mathrm{T}} \mathbf{e} \, \mathrm{d}S. \tag{6}$$

Then, equation (5) becomes

$$q(t) = \sum_{e} \mathbf{U}^{(e)\mathrm{T}} \mathbf{Q}^{(e)} G^{(e)} = \mathbf{U}^{\mathrm{T}} \mathbf{Q} \mathbf{G}, \tag{7}$$

where $\mathbf{G}$ is the vector whose element is the spatial gain $G^{(e)}$ of each element. By decomposing the nodal d.o.f vector $\mathbf{U}$ into the linear combination of eigenvectors, the electric charge induced in this transducer is expressed as the sum of the electric charges induced by each mode shape. In modal decomposition, modal reduction was used to consider only the lowest N modes:

$$q(t) = \mathbf{U}^{\mathrm{T}} \mathbf{Q} \mathbf{G} = \sum_{k=1}^{N} (\boldsymbol{\phi}_k^{\mathrm{T}} \mathbf{Q} \mathbf{G}) \eta_k(t). \tag{8}$$

The electric charge induced by the kth mode shape was defined as

$$q_k = \boldsymbol{\phi}_k^{\mathrm{T}} \mathbf{Q} \mathbf{G}. \tag{9}$$

Then, equation (8) becomes

$$q(t) = \sum_{k=1}^{N} q_k \eta_k(\mathrm{t}) = \mathbf{B}_S^{\mathbf{T}} \boldsymbol{\eta}_R, \tag{10}$$

where $\mathbf{B}_s = [q_1 \; q_2 \; \ldots q_N]$, and $\boldsymbol{\eta}_R$ is the modal displacement vector.

Due to the reciprocity [4], the actuation force for the kth mode is also q_k when the same sensor is used as an actuator if the electric charge induced by the kth mode shape is q_k. Therefore, the equation of motion of the integrated structure in modal co-ordinate system becomes

$$\ddot{\boldsymbol{\eta}}_R + \mathbf{c}_R \dot{\boldsymbol{\eta}}_R + \boldsymbol{\Lambda}_R \boldsymbol{\eta}_R = \mathbf{B}_a V_a, \tag{11}$$

where $\mathbf{c}_R = \mathrm{diag}(2\zeta_1\omega_1, \; \ldots, 2\zeta_N\omega_N)$, $\boldsymbol{\Lambda}_R = \mathrm{diag}(\omega_1^2, \; \ldots, \omega_N^2)$. $\mathbf{V}_a$ is the voltage applied to the actuator, and $\mathbf{B}_a$ is the modal actuation force vector per unit voltage defined by equation (10) and the reciprocity.

2.3. OPTIMIZATION OF SPATIAL GAIN DISTRIBUTION

Optimization of the spatial gain distribution vector $\mathbf{G}$ in equation (7) to create the modal transducer for the jth mode can be represented in the constrained optimization problem of the form

$$\begin{aligned} &\text{maximize} \quad |q_j|^2 = \mathbf{G}^{\mathrm{T}} \mathbf{Q}^{\mathrm{T}} \boldsymbol{\phi}_j \boldsymbol{\phi}_j^{\mathrm{T}} \mathbf{Q} \mathbf{G} \\ &\text{subject to} \quad \boldsymbol{\Phi}_R^{\mathrm{T}} \mathbf{Q} \mathbf{G} = \mathbf{0}, \end{aligned} \tag{12}$$

where $\boldsymbol{\Phi}_R$ was the modal matrix which consists of eigenvectors except the jth one. The constraint equation in equation (12) can be eliminated by expressing the spatial gain

distribution vector $\mathbf{G}$ as the linear combination of null space basis of $\mathbf{\Phi}_R^{\mathrm{T}}\mathbf{Q}$:

$$\mathbf{G} = \sum_{i=1}^{m} \boldsymbol{\psi}_i \alpha_i = \mathbf{\Psi}\boldsymbol{\alpha}, \tag{13}$$

where m is the nullity of $\mathbf{\Phi}_R^{\mathrm{T}}\mathbf{Q}$, $\mathbf{\Psi}$ is the null space basis matrix of $\mathbf{\Phi}_R^{\mathrm{T}}\mathbf{Q}$, and $\boldsymbol{\alpha}$ is the coefficient vector. Substituting equation (13) into equation (12), the constrained optimization problem of equation (12) can be converted into the unconstrained optimization problem in the form

$$\text{maximize} \quad \boldsymbol{\alpha}^{\mathrm{T}}\mathbf{\Psi}^{\mathrm{T}}\mathbf{Q}^{\mathrm{T}}\boldsymbol{\phi}_j\boldsymbol{\phi}_j^{\mathrm{T}}\mathbf{Q}\mathbf{\Psi}\boldsymbol{\alpha}. \tag{14}$$

To prevent the norm of vector $\mathbf{G}$ from increasing infinitely, the following constraint was imposed:

$$\|\mathbf{G}\|^2 = \boldsymbol{\alpha}^{\mathrm{T}}\mathbf{\Psi}^{\mathrm{T}}\mathbf{\Psi}\boldsymbol{\alpha} = \mathbf{1}. \tag{15}$$

From Rayleigh's inequality [11], the solution of the optimization problem, equation (14) with the constraint equation (15) is the eigenvector $\boldsymbol{\alpha}_{max}$ corresponding to the maximum eigenvalue λ_{max} of the eigenvalue problem:

$$(\mathbf{\Psi}^{\mathrm{T}}\mathbf{Q}^{\mathrm{T}}\boldsymbol{\phi}_j\boldsymbol{\phi}_j^{\mathrm{T}}\mathbf{Q}\mathbf{\Psi})\boldsymbol{\alpha} = \lambda(\mathbf{\Psi}^{\mathrm{T}}\mathbf{\Psi})\boldsymbol{\alpha}. \tag{16}$$

From equation (13), the optimal spatial gain distribution $\mathbf{G}_{opt}$ of the modal transducer for the jth mode is

$$\mathbf{G}_{opt} = \mathbf{\Psi}\boldsymbol{\alpha}_{max}. \tag{17}$$

Multi-mode modal transducers can be also obtained by the linear combination of modal transducers for each target mode.

Using this concept, one can obtain the optimal spatial gain distribution required to create the modal transducer in two-dimensional structures with arbitrary geometry and boundary conditions.

3. DESIGN OF MODAL TRANSDUCERS USING MULTI-LAYERED PVDF FILM

For the experimental realization of spatial gain distribution, one could vary the polarization profile of PVDF film by applying a spatially varying electric field during the poling procedure. But this procedure was impractical. Therefore, as a practical means for implementing the spatial gain distribution, the gain distribution was approximated by optimizing the electrode patterns, the lamination angles, and the poling directions of the multi-layered PVDF transducer. This corresponds to the approximation of a continuous function using discrete values.

In the case of single-layered PVDF film, the gain was one in the surface segment with an effective electrode, and zero in the segment without an effective electrode. Therefore, optimization of the electrode pattern was equivalent to approximating the optimal gain distribution using discretized values, i.e., $\{1, 0\}$.

In the case of multi-layered PVDF films, not only the electrode pattern and lamination angle but also the poling direction of each layer was an important design parameter. For example, if the relative poling directions of two layers of PVDF films with the same

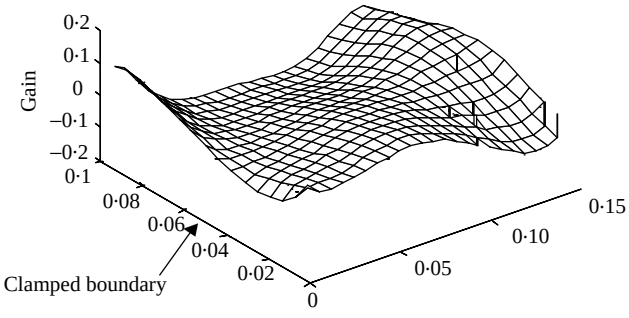

Figure 1. Optimal gain distribution for mode 4 transducer.

electrode patterns and lamination angles were opposite, then the electric charge induced from two layers cancel out each other. If the relative poling directions were the same, then the total induced charge becomes twice the amount of the electric charge induced from a single layer. Therefore, optimization of each layer's electrode pattern corresponds to the approximation of optimal gain distribution using discretized values $\{2, 1, 0\}$ in the case of same poling directions, and $\{1, 0, -1\}$ in the case of opposite poling directions.

For a demonstration of the effect of relative poling directions of multi-layered PVDF films, a modal transducer for the fourth mode of clamped composite plate with $[\pm 45^\circ]$ lay-up angles was designed. Three types of modal transducers, namely, single layer (SP), two layers with the same poling directions (SPP), and two layers with opposite poling directions (SPN), were designed with lamination angles of each PVDF film fixed to 0°.

In the design procedure, the electric charge induced from the fourth mode shape was maximized, whereas charges from other modes were minimized. Thus, the maximization problem was

$$\text{maximize} \frac{|q_4|}{\max(|q_k|)}, \quad k = 1, \cdots, N, \quad k \neq 4, \tag{18}$$

where q_k is the charge induced from the kth mode shape, as defined in equation (9), and the lowest five modes are considered in the modal reduction, i.e., $N = 5$.

The electrode pattern of each PVDF layer was optimized according to equation (18) by setting the electrode of each segment to be on or off [9]. A genetic algorithm [12], suitable for this kind of discrete optimization problem, was used as an optimization scheme.

Figure 1 shows the optimal spatial gain distribution for the fourth mode transducer that was obtained using the method proposed in the previous section.

Parts (a–c) of Figure 2 are the optimized electrode patterns of single layer (SP), two layers with the same poling directions (SPP), and two layers with opposite poling directions (SPN) respectively. In Figure 2, the left-hand side is the clamped edge, and the optimal gain distribution contour was also plotted for comparison.

In the case of SP, the optimized electrode pattern coincides with the positive region of the optimal gain distribution contour. SPP also shows a similar trend. However, the electrodes of both layers remain active in the region where relatively high positive gain was required, and the electrode of only one layer remains active where relatively low positive gain was required. In the case of SPN, the optimized electrode pattern of the layer with negative poling directions coincides with the negative gain region of the contour, while that of the layer with positive poling directions coincides with the positive region.

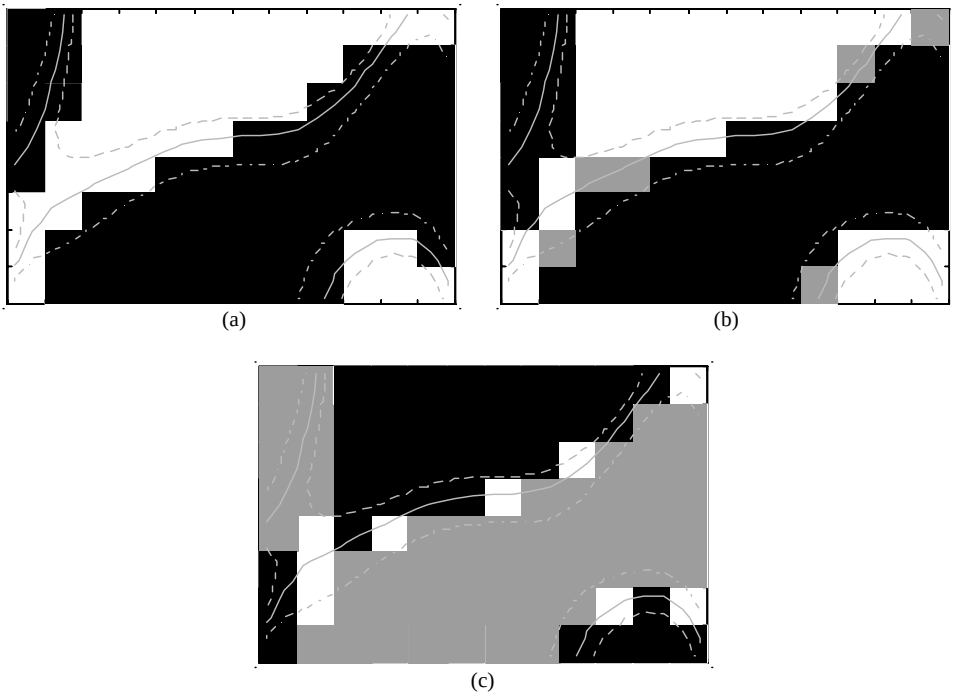

Figure 2. (a) Optimized electrode pattern for mode 4 sensor (SP): ■, poling 1; ———, zero; – – –, positive; – – –, negative. (b) Optimized electrode pattern for mode 4 sensor (SPP): ■, poling 2; ▩, poling 1; ———, zero; – – –, positive; – – –, negative. (c) Optimized electrode pattern for mode 4 sensor (SPN): ■, poling 1; ▩, poling 1; ———, zero; –·–·–, positive; – – –, negative.

TABLE 1

Performance indices and induced charges of the optimized mode 4 *transducer*

	SP	SPP	SPN
1st mode	− 1·6088e − 4	3·5137e − 4	− 3·4587e − 5
2nd mode	2·7488e − 4	4·1560e − 4	6·6927e − 5
3rd mode	5·6768e − 4	− 9·6412e − 4	2·2909e − 4
4th mode	− 1·9699e − 3	− 3·6753e − 3	2·5303e − 3
5th mode	5·6638e − 4	9·6005e − 4	− 2·2812e − 4
Performance index	3·47	3·81	11·05

The induced charge from each mode shape, defined in equation (9), and performance indices of the optimized modal transducers, defined in equation (18), are listed in Table 1. SPN shows the best performance. Optimal gain distribution for the fourth modal transducer consists of almost equal amounts of both the positive gain region and the negative gain region. Therefore, in the approximation of this optimal gain distribution, the case with one positive gain and one negative gain (SPN) was more efficient than the case with two different positive gains (SPP).

When the multi-layered PVDF films were used, we could design the modal transducer with better performance because it approximates the optimal gain distribution in a more refined manner than a single-layer case. The relative poling direction of each layer affects the performance of the multi-layered PVDF transducer.

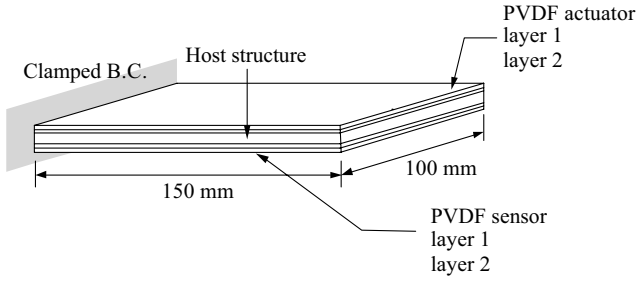

Figure 3. Schematic view of the specimen.

4. APPLICATION TO THE ACTIVE VIBRATION CONTROL OF A COMPOSITE PLATE

For an experimental demonstration, a modal sensor and actuator for the first and the second modes of a cantilevered composite plate with $[\pm 45^\circ]$ lay-up angles was designed using two layers of PVDF films on each side. The experimental set-up was established for the active vibration control. Figure 3 shows the schematic view of the structure used in this study. Through finite element analysis, the natural frequencies up to the fifth mode of the integrated structure were 12·9, 60·6, 78·9, 179·2, and 208·8 Hz respectively. As the second and third natural frequencies were closely located, it was difficult to minimize the signal from the third mode without phase lag using a time-domain filter [13]. In this case, the distributed modal transducer, a kind of filter in the spatial domain, can be applied effectively.

4.1. SENSOR AND ACTUATOR DESIGN CRITERIA

As mentioned before, the pattern optimization process is an approximation procedure. So it was impossible to make uncontrolled modes completely unobservable. The sensor was designed to minimize observation spillover due to the residual modes. Electric charges induced from residual modes (third–fifth) were minimized, whereas those from the control modes (first–second) were maximized. The performance index to be maximized was

$$J_{sensor} = \frac{\min(|\mathbf{\Phi}_c^{\mathrm{T}}\mathbf{Q}\mathbf{P}|)}{\max(|\mathbf{\Phi}_u^{\mathrm{T}}\mathbf{Q}\mathbf{P}|)}, \tag{19}$$

where $\mathbf{\Phi}_c^{\mathrm{T}}\mathbf{Q}\mathbf{P}$ and $\mathbf{\Phi}_u^{\mathrm{T}}\mathbf{Q}\mathbf{P}$ are the electric charges induced from the control modes and from the residual modes, respectively, and $\mathbf{P}$ is the vector representing the electrode pattern. $\mathbf{P}(i) = 1$ if the ith electrode segment of the structure was *on*, and $\mathbf{P}(i) = 0$ if the electrode segment was *off*.

In the actuator design, only the control modes were considered because the modal sensor eliminated the instability caused by the residual modes. The actuator was designed to minimize the system energy in the control modes under a given initial condition. Details about the actuator design criterion can be found in the previous work [9].

4.2. GENETIC ALGORITHM

As already described, a genetic algorithm was used for the optimization of each PVDF layer's electrode pattern and lamination angle. Optimization of the electrode pattern, which

TABLE 2

The binary string representation of the lamination angle

Lamination angle (deg)	Binary string
− 90	00000
− 80	00001
:	:
0	10000
5	10001
10	10010
:	:
80	11111

determines whether an electrode segment was *on* or *off*, was in itself a discrete problem. Thus, a genetic algorithm can easily deal with it. However, the optimization of lamination angles is not a discrete problem, but rather a continuous one. So to handle the problem using a genetic algorithm, discretization of the lamination angle was required. The continuous lamination angle between -90° and $+90^\circ$ was encoded into discrete values using binary 5-bit strings. There were 36 discrete values if the lamination angle was divided at intervals of 5°. But binary 5-bit strings can represent only 32 ($=2^5$) discrete values. So the lamination angle between -70° and $+70^\circ$ was divided at intervals of 5° and the rest at intervals of 10°, thus making a total of 32 discrete values. Table 2 shows the binary string representation of the lamination angle.

Since each layer consists of 96 (12×8) electrode segments and its lamination angle was encoded using binary 5-bit strings, each layer has a total of 101 binary design parameters.

4.3. DESIGN RESULTS

The sensor and actuator have been designed for the cases of two-layer PVDF films with the same poling directions (denoted as SPP for the sensor and APP for the actuator), and two-layer PVDF films with opposite poling directions (denoted as SPN for the sensor and APN for the actuator). The performances of the optimized transducers were compared with those of the transducers, which are doubly layered with the optimized single layer (denoted as SP2 for the sensor and AP2 for the actuator).

The optimized lamination angles, modal-induced charges, and performance indices of the PVDF sensors are listed in Table 3. Figure 4 gives the optimized electrode patterns of each layer of SPP, where black region was the active electrode. The left-hand edge of the figure was clamped. From Table 3, distinctions in the modal-induced charges can be observed between the control modes and the residual modes. It was noted that SPP shows better performance than SPN. It can be concluded from this case that the sensor with two different positive gains (SPP) was more efficient for approximating the optimal gain distribution than the one with one positive gain and one negative gain (SPN). Since the performance of SPP was much better than that of SP2, it was clear that the electrode patterns and the lamination angles of each layer must be optimized separately to achieve the most efficient multi-layered PVDF transducer. Therefore, SPP was chosen for the experiment.

The optimized lamination angles and modal forces of the PVDF actuators are listed in Table 4. Figure 5 shows the optimized electrode patterns of each layer of APP. APP, which shows the largest modal force for the first mode, was chosen for the experiment.

TABLE 3

Optimized lamination angles and resulting modal-induced charges of two-layer sensors

	Poling direction Layer 1 Layer 2	Lamination angle Layer 1 Layer 2	Induced charge 1st	2nd	3rd	4th	5th	Performance index
SPP	+	−15°	−4·7541e−4	6·0953e−4	2·3893e−6	−8·9009e−8	2·5787e−6	184·36
	+	−0°						
SP2	+	−15°	−5·3867e−4	9·3584e−4	7·1588e−5	6·3716e−6	−1·4420e−4	3·74
SPN	+	35°	−2·7604e−4	−2·8562e−4	4·2089e−8	1·8455e−6	−4·1661e−6	66·26
	−	0°						

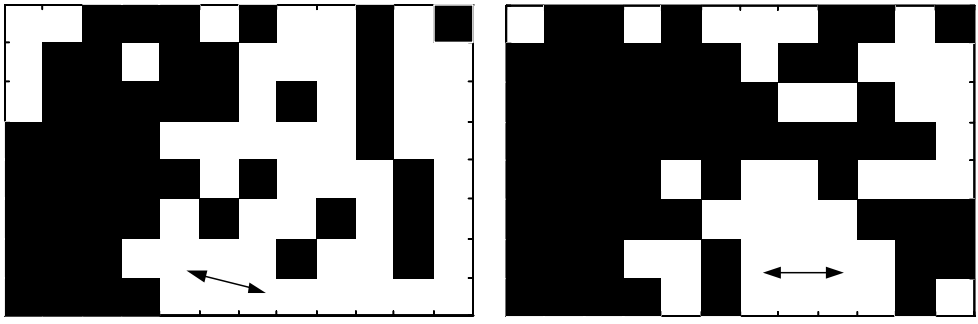

(a) (b)

Figure 4. Electrode pattern of the SPP (a) layer 1, (b) layer 2.

TABLE 4

Optimized lamination angles and resulting modal forces of two-layer actuators

	Poling direction Layer 1 Layer 2	Lamination angle Layer 1 Layer 2	Modal force 1st	2nd
APP	+	− 20°	6·3630e − 4	− 1·7477e − 3
	+	− 20°		
AP2	+	− 30°	4·7224e − 4	− 2·3001e − 3
APN	+	65°	2·9945e − 4	8·1910e − 4
	−	− 20°		

5. THE EXPERIMENT

5.1. EXPERIMENTAL SET-UP

The experiment was carried out to show the performance of the designed modal transducers and integrated structures. Figure 6 shows the block diagram of the total system. The LQG method [14] was used as a control law. The charge amplifier gain was set to 10^8

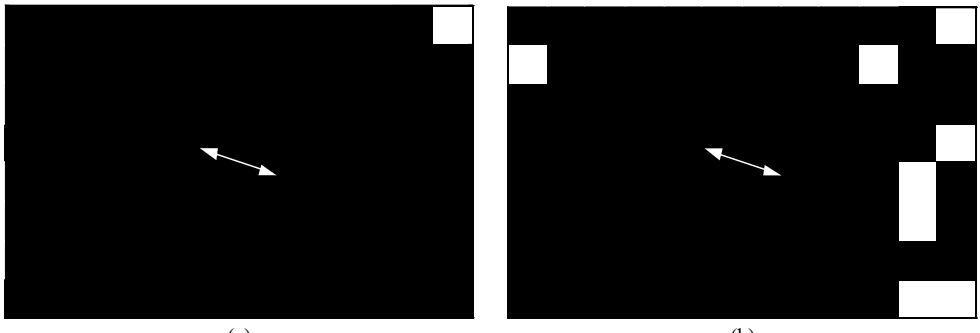

Figure 5. Electrode pattern of the APP (a) layer 1, (b) layer 2.

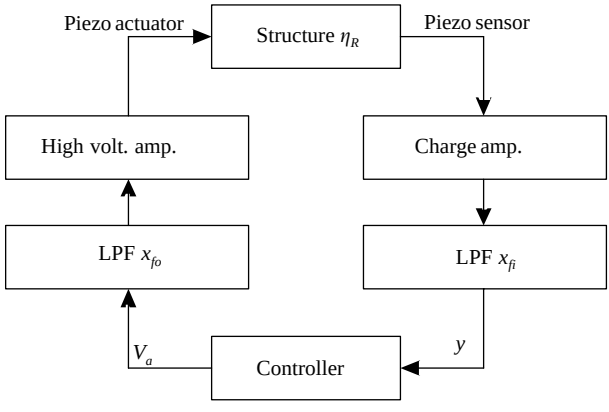

Figure 6. Block diagram of the total system.

V/F. The cutoff frequency of the anti-aliasing low-pass filter was 100 Hz. A second order Butterworth filter was used. The sensor signal was digitally sampled 5000 times per second at the A/D converter just before the controller. The control signal from the controller was applied to the actuator through the low-pass filter and the high-voltage amplifier. The gain of the high-voltage amplifier was set to 100 V/V.

The excitation force by the impact hammer and the sensor signal from the charge amplifier were processed by using the fast Fourier transform analyzer to yield the transfer function of the integrated structure.

5.2. EXPERIMENTAL RESULTS AND DISCUSSION

The experimentally obtained transfer functions of the sensor and the actuator are shown in Figure 7(a) and 7(b), respectively. In Figure 7(a), the signals from the residual modes are smaller than those from the controlled modes by an amount of 19 dB. Therefore, this sensor can be used effectively for the minimization of the observation spillover due to uncontrolled modes. The actuator may cause control spillover since Figure 7(b) shows that this actuator has relatively large actuation forces for the residual modes. But using modal sensor prevented the instability of the residual modes.

The closed-loop transfer function of our integrated structure was obtained during real-time control and is shown in Figure 8. We can find the magnitude reduction in control

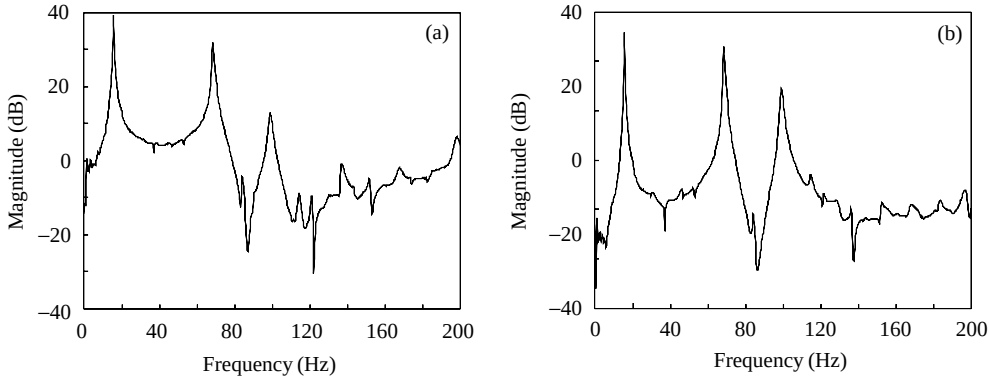

Figure 7. Open-loop transfer function of (a) the optimized sensor (SPP), (b) the optimized actuator (APP).

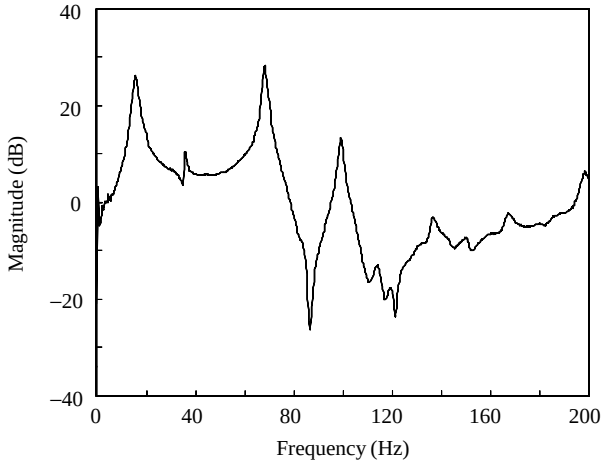

Figure 8. Closed-loop transfer function of the integrated structure.

modes. The modal peaks of the first and second modes were reduced by amounts of 13 and 4 dB respectively. Figure 9 shows the time response of the open- and closed-loop systems. Settling time was reduced to 25% compared with that of open-loop system.

6. CONCLUSION

This paper presents a method based on finite element discretization for optimizing the spatial gain distribution of PVDF film to create the modal transducer for specific modes. Using this concept, one can design a modal transducer for a two-dimensional structure having arbitrary geometric shape and boundary conditions. As a practical means for implementing this optimal gain distribution without repoling the PVDF film, the gain distribution was approximated by optimizing the electrode patterns, lamination angles, and relative poling directions of the multi-layered PVDF transducer.

For an experimental demonstration, a modal sensor for the first and second modes of the cantilevered composite plate was designed using two layers of PVDF film. The

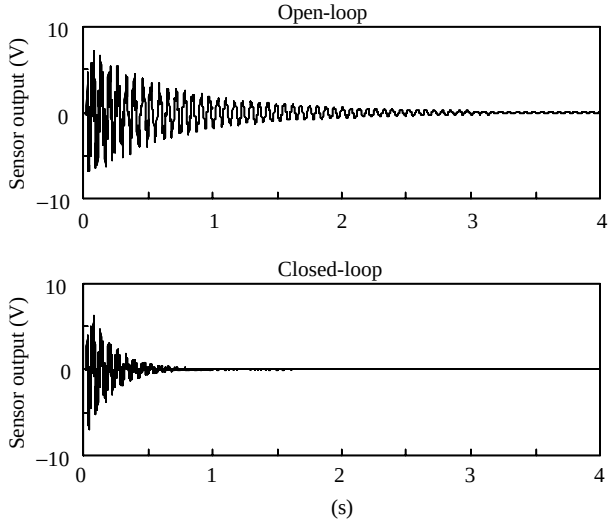

Figure 9. Open- and closed-loop time response of the integrated structure.

experimental results show that the signals from the residual modes are successfully reduced using the optimized multi-layered PVDF sensor. The real-time vibration control of integrated smart structure was successfully realized.

ACKNOWLEDGMENTS

The research was supported in part by a grant from the BK-21 Program for Mechanical and Aerospace Engineering Research at Seoul National University. And the research was supported in part by the Ministry of Science and Technology through National Research Laboratory Programs (Contract number 00-N-NL-01-C-026).

REFERENCES

1. M. J. BALAS 1978 *IEEE Transactions on Automatic Control* **23**, 673–679. Feedback control of flexible systems.
2. J. L. FANSON and T. K. CAUGHEY 1990 *American Institute of Aeronautics and Astronautics Journal* **28**, 717–724. Positive position feedback control for large space structures.
3. L. MEIROVITCH and H. BARUH 1985 *Journal of Guidance and Control*, **8**, 707–716. The implementation of modal filters for control of structures.
4. C.-K. LEE 1992 in *Intelligent Structural Systems* (H. S. Tzou and G. L. Anderson editors), 75–167. Piezoelectric laminates: theory and experiments for distributed sensors and actuators. Dordrecht: Kluwer Academic Publishers.
5. S. E. BURKE and J. E. HUBBARD Jr. 1991 *Journal of Acoustical Society of America* **90**, 937–944. Distributed transducer vibration control of thin plates.
6. S. E. MILLER, Y. OSHMAN and H. ABRAMOVICH 1996 *American Institute of Aeronautics and Astronautics Journal* **34**, 1868–1875. Modal control of piezolaminated anisotropic rectangular plates. Part 1: modal transducer theory.
7. J. M. SULLIVAN, S. E. BURKE and J. E. HUBBARD 1995 *American Institute of Aeronautics and Astronautics Paper*, Vol. 95–1119. Experimental demonstration of active broadband vibration suppression of a rectangular plate using gain-weighted, shaped distributed transducer.

8. H. S. TZOU, J. P. ZHONG and J. J. HOLLKAMP 1994 *Journal of Sound and Vibration*, **177**, 363–378. Spatially distributed orthogonal piezoelectric shell actuators: theory and application.
9. J.-K. RYOU, K.-Y. PARK and S.-J. KIM 1998 *American Institute of Aeronautics and Astronautics Journal* **36**, 227–233. Electrode pattern design of piezoelectric sensors and actuators using genetic algorithms.
10. Y. K. CHEUNG, S. H. LO and Y. T. LEUNG 1996 *Finite Element Implementation*. Oxford: Blackwell Science.
11. G. STRANG 1988 *Linear Algebra and It's Application*. New York: Harcourt Brace & Company.
12. D. E. GOLDBERG 1989 *Genetic Algorithm in Search*. Reading, MA: Addison-Wesley. Optimization and machine learning.
13. S. A. COLLINS, D. W. MILLER and A. H. VON FLOTOW 1994 J*ournal of Sound and Vibration*, **173**, 471–501. Distributed sensors as spatial filters in active structural control.
14. J. M. MACIEJOWSKI 1989 *Multivariable Feedback Design*. Reading, MA: Addison-Wesley.